



Short communication

MnO₂ film with three-dimensional structure prepared by hydrothermal process for supercapacitor

Dongliang Yan^a, Zilong Guo^a, Guisheng Zhu^a, Zhaozhe Yu^a, Huarui Xu^{a,*}, Aibing Yu^b

^a School of Materials Science and Engineering, Guilin University of Electronic Technology, Guilin 541004, PR China

^b School of Materials Science and Engineering, University of New South Wales, Sydney, NSW 2052, Australia

ARTICLE INFO

Article history:

Received 7 June 2011

Received in revised form 31 August 2011

Accepted 13 October 2011

Available online 20 October 2011

Keywords:

Manganese dioxide film

3D structure

Hydrothermal method

Supercapacitor

ABSTRACT

A novel three-dimensional (3D) porous MnO₂ film has been deposited onto a foamed nickel with another 3D structure by a hydrothermal method using potassium permanganate and sodium dodecylsulfate under neutral condition. Characterized by powder X-ray diffraction, scanning electron microscopy and thermal analysis, so formed 3D structure film is composed of nanosheets or nanofibers and has an amorphous and hydrous nature. The high specific capacitance of 241 F g⁻¹ is observed at the current density of 1 A g⁻¹, investigated by means of cyclic voltammetry and constant current charge–discharge cycling in 1 M Na₂SO₄ aqueous solutions. The film shows a good reversibility, power characteristics and cycling stability. It is promising for supercapacitor application.

Crown Copyright © 2011 Published by Elsevier B.V. All rights reserved.

1. Introduction

Supercapacitors, also known as ultracapacitors or electrochemical supercapacitors, are a unique electrochemical device with high power density, high charge–discharge cycle life and high energy efficiency. The energies stored in supercapacitors mainly come from either the electrical double-layer capacitance of various carbonaceous materials with high specific surface areas or the Faradaic pseudo-capacitance of electroactive materials with several oxidation states [1]. The former is based on charge separation at the electrode/solution interface, whereas the latter is based on the Faradaic redox reactions occurring within the active electrode materials. Many noble or transition metal oxides can show pseudo-capacitive behavior, and among different metal oxides, ruthenium oxides have been extensively studied as active electrode materials for supercapacitor because they exhibit a capacitance as high as 863 F g⁻¹ in aqueous acidic electrolytes [2]. However, the high cost of ruthenium has limited its commercial application. Because of its low cost, less toxicity and abundance in nature, manganese oxide has been considered to be the most attractive alternative to RuO₂. The methods used for the fabrication of manganese oxide electrodes are mainly based on the deposition of thin films to form thin-film electrodes or pasting manganese oxide powders

mixed with binders and conductive additives on conductive current collectors to form powder-based composite electrodes [3]. Because of their efficient size-related performance in comparison with powder-based counterparts, nano-structured MnO₂ thin films have been explored as possible supercapacitors in recent years [4].

So far, various methods have been developed to prepare MnO₂ films, including sol–gel method [5], anodic deposition [6], cathodic deposition [3], and other chemical or physical methods [7]. Compared to these methods, hydrothermal method is attractive because of its operational simplicity, good coating efficiency and capability for large-scale production. And what's more, deposition on a 3D structure is an additional advantage of the hydrothermal deposition method, where a thin film can be deposited on all surfaces of a substrate [8]. Recently, as a result of their large surface area and short ion diffusion distance comparing to 2D plate electrodes, 3D structure electrodes have attracted a lot of attention in both fundamental and applied research [9].

In the literatures, sodium dodecylsulfate (SDS) was used to prepare MnO₂ in the hydrothermal process; however it must be in a perchloric acid medium [10,11]. Obviously such a reactor must be endure the corrosion of acid and thus expensive. In this paper, we report a hydrothermal method to prepare 3D MnO₂ film upon nickel foam with another 3D structure using potassium permanganate (KMnO₄) and SDS under neutral condition. The structures of the resulting films were characterized by XRD, SEM and TG–DSC. The electrochemical properties of this MnO₂ film for supercapacitor were investigated by cyclic voltammetry and galvanostatic charge/discharge in neutral aqueous Na₂SO₄ electrolyte.

* Corresponding author. Tel.: +86 773 2291159; fax: +86 773 2191903.

E-mail addresses: xuhuarui@163.com, huaruiXu@guet.edu.cn (H. Xu).

2. Experimental

3D structure nickel foam (thickness: 1.8 mm, pore density: 110 ppi) was first degreased with acetone and water, then etched in a 0.1 M HCl solution at room temperature for 10 min, and finally degreased with water in an ultrasonic bath.

Commercial KMnO_4 and SDS (from Shanghai Chemical Corp.) of analytical grade were directly used as the starting materials, without further purification. SDS (0.04 g) was dissolved in 10 mL deionized water, and then 20 mL of 0.02 g mL^{-1} KMnO_4 solution was added drop by drop into it and stirred for 15 min to obtain a homogeneous solution. Subsequently, the well-mixed solution was transferred into a 40 mL autoclave. The cleaned Ni foam was put into the autoclave and stored in the sealed autoclave at 130°C for 10 h. The autoclave was then cooled to the room temperature and the blackened foamed Ni was washed with deionized water several times before drying at 50°C for 24 h. The amount of deposited MnO_2 film on the substrate was determined by dissolving the film in an $\text{H}_2\text{O}_2/\text{HNO}_3$ mixture and using inductively coupled plasma/atomic emission spectrometry (ICP/AES) [6,12]. The surface area of the film electrode is 1 cm^2 and the typical loading of MnO_2 is about 1.03 mg.

A part of the hydrothermal deposit was carefully scraped from the nickel foam and analyzed with X-ray diffraction (XRD, Rigaku Geigerflex D/Max 2200) and TG/DSC (Netzsch STA-449F3) [4]. For the XRD studies, the deposit was also annealed in air at various temperatures for 2 h. The microstructures of the obtained oxide films were evaluated by means of a FEI field emission scanning electron microscopy (FESEM, FEI, Quanta 400FEG). The electrochemical measurements were carried out in an electrochemical workstation (CHI 660A) using a conventional three-electrode electrochemical cell with a 1 M Na_2SO_4 aqueous solution as electrolyte. The MnO_2 film was used as the working electrode, and a Pt-sheet and saturated calomel electrode (SCE) were used as counter and reference electrodes, respectively.

3. Results and discussion

Fig. 1(a) shows the optical photographs of the foamed nickel before (left) and after (middle) the deposition of the MnO_2 film. The shiny Ni foam became dark black in color after 10 h of treatment, suggesting the formation of MnO_2 on the nickel substrate. In order to investigate the stability of the Ni foam, we also performed some controlled experiments where the conditions were kept the same except that KMnO_4 and SDS were not added. The results showed that no changes both in color (Fig. 1(a), right) and weight were detected, indicating the foamed nickel was stable under hydrothermal conditions.

Fig. 1(b) and (c) shows the surface morphologies of foamed nickel before and after deposition. Before deposition, Ni foam showed a smooth and typical silvery metallic luster surface with a 3D structure and $\sim 300 \mu\text{m}$ pore size. In contrast, after deposited, the nickel foam presented a rough and lusterless appearance, indicating that a film may grow on the nickel foam. The morphology of the deposited film was further characterized by SEM. As shown in Fig. 1(d), the deposited film was composed of intertwined nanosheets or nanofibers with diameter in the range of 5–10 nm and length in the order of 100–200 nm. It was also found the deposited film was porous with a 3D structure and $\sim 20 \text{ nm}$ pore size, which would be wide enough for electrolyte used for supercapacitor application. This 3D structure could provide larger surface area for active materials to contact the electrolyte and was expected to produce high SC values when used for capacitor application. Similar morphologies were reported previously for amorphous nanostructured hydrous manganese oxides made by potentiodynamic deposition [13].

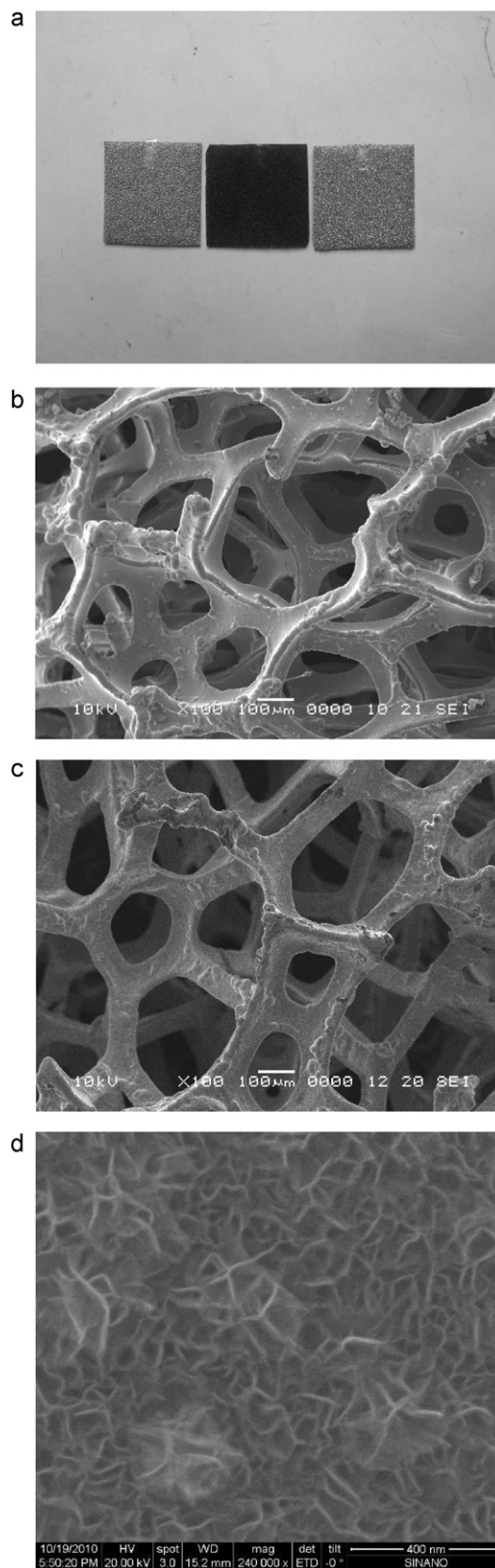


Fig. 1. (a) Photos showing the nickel foam before (left) and after (middle) deposition, and hydrothermal treatment in the absence of KMnO_4 and SDS (right); (b) SEM overview of Ni foam before deposition; (c) SEM overview of Ni foam after deposition; and (d) SEM photographs of as-prepared MnO_2 film.

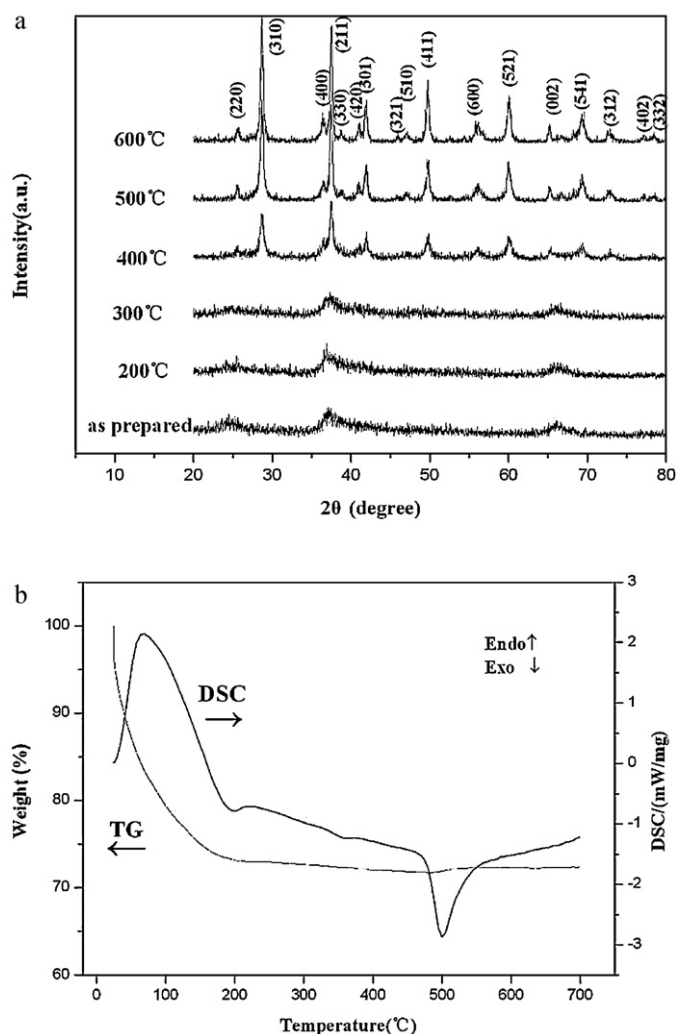


Fig. 2. (a) XRD patterns of the as-prepared MnO₂ and those heat-treated at various temperatures for 2 h in air and (b) TG/DSC curve for the deposits.

To confirm the deposited materials, a part of deposited materials was carefully scraped from nickel foam for the characterization. Fig. 2(a) shows the XRD patterns of the fresh deposits and those annealed in air at different temperatures. The as-prepared manganese oxide exhibited a very broad diffraction peak around $2\theta \sim 37^\circ$, indicating the deposits had an amorphous structure. The increase in intensity of this peak with temperature showed a gradual transformation to crystalline phase. After annealing at 400 °C, a highly crystalline sample was obtained and the pattern matched well with α -MnO₂ (JCPDS NO. 44-0141). Fig. 2(b) shows the TG/DSC curve of the deposits in the temperature range from the room temperature to 700 °C. The sharp weight loss occurred below 100 °C and this could be attributed to the desorption of physically adsorbed water. As the temperature increased to 200 °C, the rate of weight loss decreased slightly and this was caused by the dehydration of crystalline water. According to the TG/DSC curve, the total weight loss of adsorbed water and crystalline water was 28.3% and the presence of water in the MnO₂ structure was generally believed to be favorable for electrochemical activity [14]. Usually MnO₂ would be transformed to Mn₂O₃ at about 500 °C [4,15], which was harmful to the power characteristics and cycling stability of supercapacitor. In the present work, as the temperature increased to 500 °C, the TG/DSC curve showed a slight gain in weight (about 0.57%) and a sharp exothermic peak. This weight gain was attributed to the oxygen uptake due to oxidation [16]. In addition, the MnO₂ in this case

exhibited a good thermal stability from the XRD and TG/DSC results, which is good to the power characteristics and cycling stability of supercapacitor as reported by Tsang et al. [17]. These investigators attributed the good thermal stability of MnO₂ to a high concentration of potassium (K/Mn^{-1} mole ratio = 0.251 as estimated from ICP in the present work).

From above characterization, the films deposited on the 3D Ni foam can be proved as MnO₂ with 3D structure and is composed of nanosheets or nanofibers and has an amorphous and hydrous nature. Raju [10] prepared MnO₂ by hydrothermal method using KMnO₄ and SDS in a perchloric acid medium. This strong acid condition must need expensive reactor enduring the corrosion of acid and cannot use the Ni foam as the substrate. In the present work, not using strong acid, the neutral environment could be provided a moderate, cheap and safe condition in the hydrothermal process.

A typical cyclic voltammograms of the as-prepared MnO₂ film within the potential range of 0–1 V at scan rate of 2 mV s⁻¹ is shown in Fig. 3(a) (curve 2). The CV curve showed roughly rectangular mirror images with respect to the zero-current line and there are no redox peak in the range between 0 and 1 V. The results indicated that MnO₂ film electrode prepared by the present hydrothermal method behaved as an ideal capacitor within the potential window of 0–1 V. The CV curve for bare Ni foam (curve 1 in Fig. 3(a)) was also recorded in the same electrolyte as a control, and a negligible capacitive current was observed. It suggested that Ni foam hardly showed any electrochemical capacity performance. The power characteristics of the MnO₂ film electrode were examined by changing the scan rate, and the results are shown in Fig. 3(b). They indicated that all the CVs of MnO₂ film electrode remained a rectangular-like with symmetric shape, even at a high scan rate of 200 mV s⁻¹. Hence, the MnO₂ film electrode has excellent power characteristics.

The charge–discharge behavior of the MnO₂ film was also examined by chronopotentiometry between 0 and 1 V at current density of 1 A g⁻¹, as shown in Fig. 3(c). The linear and symmetric charge/discharge curves indicated good capacitive and revisable behavior. The SC can be calculated from the charge/discharge curves according to following equation [9]:

$$SC = \frac{it}{m\Delta V} \quad (1)$$

where i is the constant discharge current, t is the time for discharge, m represents the total mass of the active material on the electrode, and ΔV is the voltage change from 1 to 0 V caused by discharge. The SC value was determined to be 241 F g⁻¹.

There are several specific capacitance data reports on hydrothermal synthesized MnO₂ powder for composite electrodes in the references [18–21]. For instance, specific capacitance of 72–168 F g⁻¹ was reported for MnO₂ prepared from hydrothermal route based on aqueous solutions of MnSO₄·H₂O and KMnO₄ [18,19]. Xu et al. [20] reported the highest specific capacitance value of 124 F g⁻¹ for hollow MnO₂ from the hydrothermal treatment of the solution of KMnO₄ and sulfuric acid with Cu scraps as a catalyst. Similarly, Tang et al. [21] synthesized α -MnO₂ nanostructures by a hydrothermal decomposition of single KMnO₄ under nitric acid conditions, and the maximum specific capacitance of 152 F g⁻¹ was obtained for the supercapacitor in a 1 M Na₂SO₄ aqueous electrolyte. Obviously, the specific capacitance value in the present work is reasonably high in comparison with these values reported for hydrothermal synthesized composite electrodes.

The long-term cycling stability of MnO₂ film electrode was investigated by chronopotentiometry at a current density of 1 A g⁻¹, and the variation of specific capacitance over 1000 cycles was depicted in Fig. 3(d). The specific capacitance decreased slightly in the initial 300 cycles and then remained constant. The film showed a loss of less than 10% of the discharge capacity after 1000

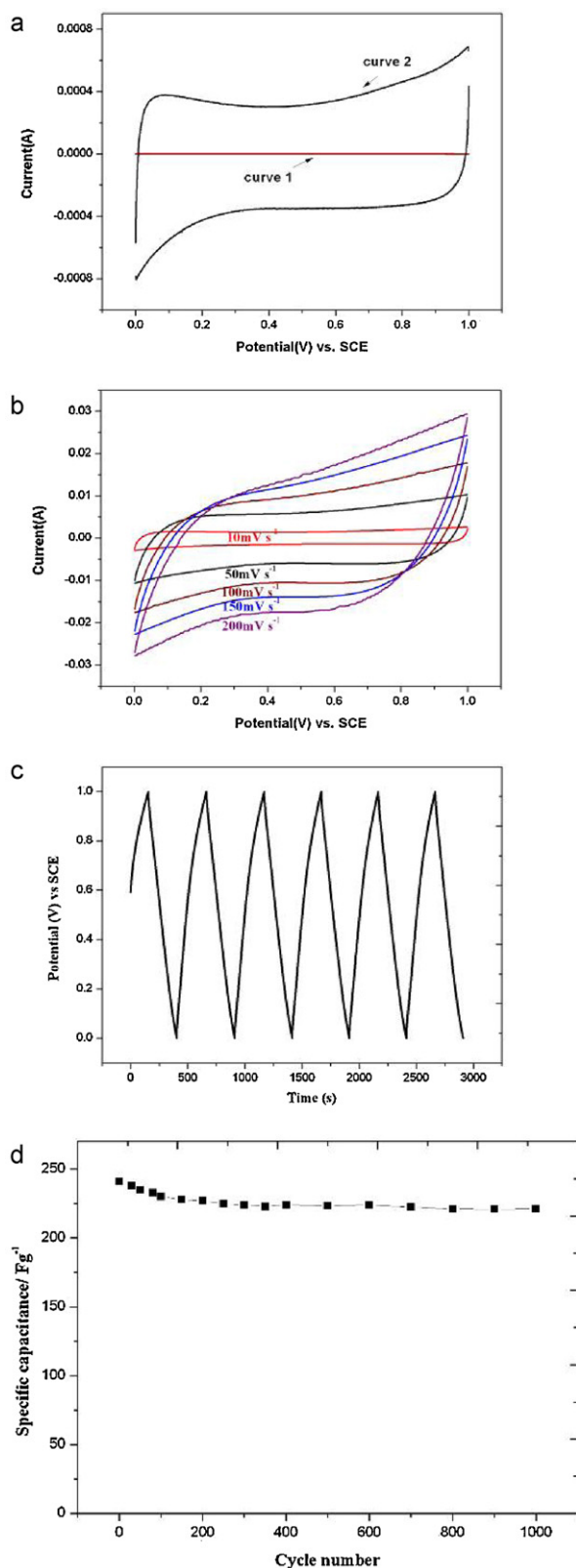


Fig. 3. (a) Cyclic voltammograms of the MnO₂ film electrode and bare nickel foam in 1 M NaSO₄ solution at a scan rate of 2 mV s⁻¹; (b) Cyclic voltammograms of the MnO₂ film electrode at different scan rates; (c) charge/discharge curve of MnO₂ film in the potential range from 0 to 1 V at 1 A g⁻¹; and (d) Cycle life of the MnO₂ film at 1 A g⁻¹.

cycles. The long-term stability suggested that the MnO₂ film was a good candidate for supercapacitor electrodes.

The excellent supercapacitive properties of the synthesized MnO₂ film could be attributed to the effective utilization of MnO₂. Different from the hydrothermal synthesized composited electrode, which were packed tightly in bulk, our MnO₂ grains were fully dispersed on foamed Ni, making every MnO₂ contact with the conductive current collector and exposing itself to electrolytes [22]. Besides, compared to 2D plate electrodes, the 3D structure of Ni foam together with the porous MnO₂ nanostructure not only facilitates the penetration of electrolytes into the whole active materials, but also shortens the ion diffusion distance [9,23,24].

4. Conclusions

A 3D structure manganese oxide film was hydrothermally deposited onto another 3D foamed nickel, using KMnO₄ and SDS as starting materials under neutral condition. The film had an amorphous and hydrous nature and exhibited the high specific capacitance of 241 F g⁻¹. The prepared MnO₂ film showed its ideal capacitive nature and high specific capacitance, and long cycle life. It had a good potential as an electrode material for supercapacitors.

Acknowledgments

This work was supported by the National Natural Science Foundation of China (Grant Nos. 21176051 and 61166008) and the Foundation of Guangxi Educational Committee of China (Grant No. 200808MS165). The authors would like to thank Professor Hongqiang Wang of Guangxi Normal University and Professor Shengkui Zhong of Guilin University of Technology for their advice and help in electrochemical tests. We also thank professor Qiangbin Wang of Suzhou Institute of Nano-Tech and Nano-Bionics for assistance with the SEM measurements.

References

- [1] H.Q. Wang, Z.S. Li, J.H. Yang, Q.Y. Li, X.X. Zhong, J. Power Sources 194 (2009) 1211–1218.
- [2] H.S. Kim, B.N. Popov, J. Power Sources 104 (2002) 52–61.
- [3] K.W. Chung, K.B. Kim, S.H. Han, Electrochem. Solid-State Lett. 8 (2005) A259–A262.
- [4] J. Wei, N. Nagarajan, I. Zhitomirsky, J. Mater. Process. Technol. 186 (2007) 356–361.
- [5] M.Q. Wu, L.P. Zhang, J.H. Gao, J. Electroanal. Chem. 613 (2008) 125–130.
- [6] S.C. Pang, M.A. Anderson, T.W. Chapman, J. Electrochem. Soc. 147 (2000) 444–450.
- [7] Y. Dai, K. Wang, J.C. Zhan, J.Y. Xie, J. Power Sources 161 (2006) 737–742.
- [8] T. Morita, Y. Wagatsuma, J. Mater. Res. 19 (2004) 1862–1868.
- [9] C. Wang, D. Wang, Q. Wang, H. Chen, J. Power Sources 195 (2010) 7432–7437.
- [10] Z. Khan Raju, Bull. Chem. Soc. Jpn. 78 (2005) 1218–1222.
- [11] X.C. Song, Y. Zhao, Y.F. Zheng, Cryst. Growth Des. 7 (2007) 159–162.
- [12] S.F. Chin, S.C. Pang, M.A. Anderson, J. Electrochem. Soc. 149 (2002) A379–A384.
- [13] K.R. Prasad, N. Miura, J. Power Sources 135 (2004) 354–360.
- [14] H.S. Kim, B.N. Popov, J. Electrochem. Soc. 150 (2003) D56–D62.
- [15] T. Shinomiya, V. Gupta, N. Miura, Electrochim. Acta 51 (2006) 4412–4419.
- [16] P. Ragupathy, H.N. Vasan, N. Munichandraiah, J. Electrochem. Soc. 155 (2008) A34–A40.
- [17] C. Tsang, J. Kim, A. Manthiram, J. Solid State Chem. 137 (1998) 28–32.
- [18] V. Subramanian, H.W. Zhu, R. Vajtai, P.M. Ajayan, B.Q. Wei, J. Phys. Chem. B 109 (2005) 20207–20214.
- [19] V. Subramanian, H.W. Zhu, B.Q. Wei, J. Power Sources 159 (2006) 361–364.
- [20] M.W. Xu, L.B. Kong, W.J. Zhou, H.L. Li, J. Phys. Chem. C 111 (2007) 19141–19147.
- [21] N. Tang, X.K. Tian, C. Yang, Z.B. Pi, Mater. Res. Bull. 44 (2009) 2062–2067.
- [22] G.W. Yang, C.L. Xu, H.L. Li, Chem. Commun. 48 (2008) 6537–6539.
- [23] S. Devaraj, N. Munichandraiah, J. Phys. Chem. C 112 (2008) 4406–4417.
- [24] J.T. Zhang, W. Chu, J.W. Jiang, X.S. Zhao, Nanotechnology 22 (2011) 125703.